

MESOSPHERIC OZONE MEASUREMENTS BY SAGE II

D. A. Chu¹ and D. M. Cunnold²¹ G & A Technical Software, Inc., Hampton, Va 23666² School of Earth and Atmospheric Sciences, Georgia Institute of Technology, Atlanta, Ga 30332**Abstract**

SAGE II observations of ozone at sunrise and sunset (solar zenith angle = 90°) at approximately the same tropical latitude and on the same day exhibit larger concentrations at sunrise than at sunset between 55 and 65 km. Because of the rapid conversion between atomic oxygen and ozone, the onion-peeling scheme used in SAGE II retrievals, which is based on an assumption of constant ozone, is invalid. A one-dimensional photochemical model is used to simulate the diurnal variation of ozone particularly within the solar zenith angle of 80° - 100°. This model indicates that the retrieved SAGE II sunrise and sunset ozone values are both overestimated. The Chapman reactions produce an adequate simulation of the ozone sunrise/sunset ratio only below 60 km, while above 60 km this ratio is highly affected by the odd oxygen loss due to odd hydrogen reactions, particularly OH. The SAGE II ozone measurements are in excellent agreement with model results to which an onion-peeling procedure is applied. The SAGE II ozone observations provide information on the mesospheric chemistry not only through the ozone profile averages but also from the sunrise/sunset ratio.

Introduction

The diurnal variation of ozone in the mesosphere has been discussed recently in several models such as Rusch and Liu (1981), Prather (1981) and Allen et al (1984). They all display a similar pattern for the ozone diurnal variations, however none of them have compared model results and measurements in the transition period such as at sunrise and sunset because of the lack of observations. SAGE II ozone measurements are however made at 90° solar zenith angle and thus provide an excellent opportunity to examine the behavior of ozone at sunrise and sunset, or more particularly the variation between sunrise and sunset (i.e. the ozone sunrise/sunset ratio), and thus to test mesospheric ozone photochemistry.

The SAGE II data we examined are for the five-year period, 1985-1990. The vertical resolution of the ozone observations is approximately 1 km. The SAGE II ozone channel is centered at 0.6 μm in the Chappuis band. The orbital period is approximately 1.5 hours which results in 30 events per day (15 sunrises and 15 sunsets). The separation of each sunrise or sunset event is approximately 24 degrees in longitude and less than one half a degree in latitude. Each retrieved ozone profile is approximately representative of the atmosphere at local sunrise or sunset but it is derived on the basis of the assumption that temporal ozone variation is not included.

A one-dimensional photochemical model is utilized to investigate the ozone variation during twilight hours. Although transport effects might be important on time scales of an hour or more the resulting ozone changes are equally as likely to be positive or negative in the tropics and should thus be averaged

out over many observations. Two types of chemical schemes were used to study the ozone diurnal variation: pure oxygen photochemistry and the photochemistry involving both odd oxygen and odd hydrogen.

The model simulations clearly show unequal sunrise and sunset ozone profiles (i.e. sunrise > sunset) at altitudes between 55 and 65 km. The SAGE II ozone profiles had also shown the differences between sunrise and sunset at that altitude range. Above 65 km the SAGE II retrieved ozone concentrations are controlled by retrieval constraints because of measurement noise (Cunnold et al, 1989; Chu et al 1989). The differences between sunrise and sunset of SAGE II ozone are found to be much larger than those modeled at 90° solar zenith angle. This paper emphasizes the ozone sunrise/sunset ratio rather than the individual sunrise or sunset profiles in order to test our understanding of mesospheric ozone chemistry during twilight and nighttime hours.

One-dimensional, time-dependent model

As already indicated above the modeling effort is focused on the behavior of ozone between sunset and sunrise. The overnight loss of odd oxygen caused by reactions between atomic oxygen and odd hydrogen radicals is included. Odd hydrogen concentrations in the mesosphere are poorly known. The twilight behavior of odd hydrogen species is therefore modeled. We have not however attempted to simulate the full diurnal cycle of ozone because this would introduce additional modeling uncertainties and SAGE II provides no information on daylight ozone concentrations in the mesosphere.

The geometry of the model is displayed in Figure 1. The chemical species abundance is a function of solar zenith angle and altitude. The coverage of the model is from 50 to 80 km and from 80° to 120° solar zenith angle. Photochemical reactions used in the model are tabulated in Table 1. Photochemical equilibrium of ozone is assumed at 80° solar zenith angle and the ozone first guess values are from the U.S. Standard Atmosphere (1976). The model time step is set equal to 2 seconds to accommodate the fast chemical time scale of atomic oxygen variations at 50 km altitude (i.e. 10 seconds). The height increment is 0.5 km which is one-half of the SAGE II vertical resolution.

In order to obtain the initial slant path ozone abundances, which are needed to compute the photodissociation rate of ozone, a Chapman function (Smith and Smith, 1972) is employed at the upper boundary (= 80 km) and at the initial state as well (i.e. = 80° solar zenith angle). Elsewhere linear interpolation is applied to the ozone concentrations at the nearest intersection of the altitude and solar zenith angle grid. The absorption cross section of ozone and solar irradiances are from Atmospheric Ozone (1985), and the cross sections of molecular oxygen in Schumann-Runge bands are from Frederick and Hudson (1960).

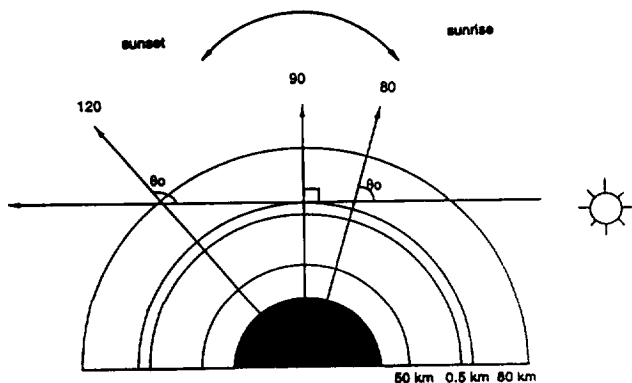


Fig.1 Model geometry used to calculate columnar ozone amounts and photodissociation rates. θ_0 indicates the local solar zenith angle of incremental contributions.

The integration procedure at sunset is straightforward and requires no iteration. Due to the model geometry (see Figure 1) the ozone column along the sunset ray contains contributions from different solar zenith angles (i.e. earlier local times for which calculations have been completed). For the sunrise ray, on the other hand, the grid points correspond to later times for which the calculations have not yet been made. To obtain the ozone profile at sunrise, the model was thus integrated starting from the nighttime ozone values until the convergence is attained. In each iteration the updated slant path columns produce updated ozone profiles. The model seeks convergence at each altitude and solar zenith angle grid point. Six iterations are typically required using a factor of 0.0001 times the ozone concentration as the convergence criterion at each grid point.

It is assumed in these calculations that ozone absorption is much larger than the effect of Rayleigh scattering. Anderson (1983) pointed out that the multiple scattering of solar radiation can be ignored at altitudes above 50 km at wavelengths less than 0.31 μm . Although it can become important at large solar zenith angles ($> 93\text{-}94^\circ$) (Noxon et al, 1979), the substantial absorption by ozone at these angles results in negligible photodissociations below 70 km altitude. At lower altitudes where the reflection of solar radiation may be strong it can also be ignored compared to the absorption by ozone. The effect due to multiple scattering and ground albedo is thus neglected, however, the singly scattered solar radiation from an infinitesimally thin layer (Solomon et al (1987)) is included.

Because of the sensitivity of the calculations to the initial ozone profile, it is important that the calculated sunrise/sunset ratio is constrained by the observed ozone profile. The initial ozone profile is therefore iterated until the calculations yield the observed ozone profile (1% difference is assumed) at sunset. It should be noted that the agreement between the calculated profile and the observed SAGE II mean profile is obtained only after the onion peel inversion procedure has been applied to the calculated time-dependent profiles.

HO_x-O_x photochemistry

Odd hydrogen compounds contribute to an overnight loss of odd oxygen through the following reactions

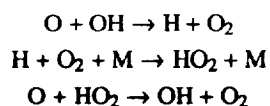


Table 1 Photochemical reactions used in the model

Reactions	Rate constants
(R1) $\text{O}_3 + h\nu \rightarrow \text{O} + \text{O}_2$	$\lambda < 0.31 \mu\text{m}$
(R2) $\text{O} + \text{O}_2 + \text{M} \rightarrow \text{O}_3 + \text{M}$	$6.0 \times 10^{-34} (300/T)^{2.3}$
(R3) $\text{O} + \text{OH} \rightarrow \text{H} + \text{O}_2$	$2.3 \times 10^{-11} \exp^{-90/T}$
(R4) $\text{O} + \text{HO}_2 \rightarrow \text{OH} + \text{O}_2$	$2.8 \times 10^{-11} \exp^{172/T}$
(R5) $\text{H} + \text{O}_2 + \text{M} \rightarrow \text{HO}_2 + \text{M}$	$1.76 \times 10^{-28} T^{-1.4}$
(R6) $\text{OH} + \text{HO}_2 \rightarrow \text{H}_2\text{O} + \text{O}_2$	8.4×10^{-11}
(R7) $\text{OH} + \text{OH} \rightarrow \text{H}_2\text{O} + \text{O}$	$4.5 \times 10^{-12} \exp^{-275/T}$
(R8) $\text{HO}_2 + \text{HO}_2 \rightarrow \text{H}_2\text{O}_2 + \text{O}_2$	$2.4 \times 10^{-14} \exp^{1250/T}$
(R9) $\text{O} + \text{O}_3 \rightarrow 2\text{O}_2$	$1.5 \times 10^{-11} \exp^{-2218/T}$
(R10) $\text{O}_2 + h\nu \rightarrow \text{O} + \text{O}$	$0.17 < \lambda < 0.25 \mu\text{m}$
(R11) $\text{H} + \text{O}_3 \rightarrow \text{OH} + \text{O}_2$	$1.4 \times 10^{-10} \exp^{-270/T}$
(R12) $\text{OH} + \text{O}_3 \rightarrow \text{HO}_2 + \text{O}_2$	$1.6 \times 10^{-12} \exp^{-940/T}$

The reaction constants are all from Allen et al, 1984 except (R2) (which is from J. Phys. Chem., Vol. 11, 1982), photodissociation rates of ozone and molecular oxygen are calculated in the model itself.

which encompass a major catalytic destruction of odd oxygen above the stratopause. The OH abundances taken from Allen et al (1984) around 1800 hr are used as initial values. The HO₂ is derived in the photochemical balance as follows

$$[\text{HO}_2] = \frac{K_3}{K_4} [\text{OH}] - \frac{K_{11} [\text{H}] [\text{O}_3]}{K_4 [\text{O}]}$$

These catalytic reactions are able to destroy atomic oxygen very efficiently and when the abundance of atomic oxygen is greater than 10^7 cm^{-3} ($\sim 1/400$ of its daytime value) a significant loss of O_x is thus expected. The equation controlling the loss of odd oxygen in this model can be written as

$$\frac{\partial [\text{O}_x]}{\partial t} = 2 J_{\text{O}_2} [\text{O}_2] - 2 K_3 [\text{O}] [\text{OH}] - 2 K_9 [\text{O}] [\text{O}_3]$$

Figure 2 depicts the variability of odd oxygen from 80° to 110° solar zenith angle between 50 and 70 km. At 70 km, approximately 35% of the initial odd oxygen is destroyed within a two hour period around sunset. A 15% loss of odd oxygen occurs before sunset and a 20% loss takes place after dark. During the period before sunset the O/O₃ ratio remains constant, with O of an order of magnitude larger than O₃. In the early part of night during which the O/O₃ ratio decreases by a factor of two, no significant increase of ozone occurs. This is because oxygen atoms are removed by O+OH catalytic reactions instead of being converted to O₃. At solar zenith angles greater than 93° (at which time O has decreased to just a factor of two larger than O₃), ozone begins to increase substantially. At 65 km altitude, the odd oxygen loss is primarily concentrated in a hour period before sunset, and the loss of odd oxygen is approximately 30%. The O/O₃ ratio however, in the same period, tends to remain a constant. At 60 km the loss of odd oxygen is 15% and only occurs before sunset. Below 60 km the loss of odd oxygen is small - only 5% at 55 km and 2% at 50 km.

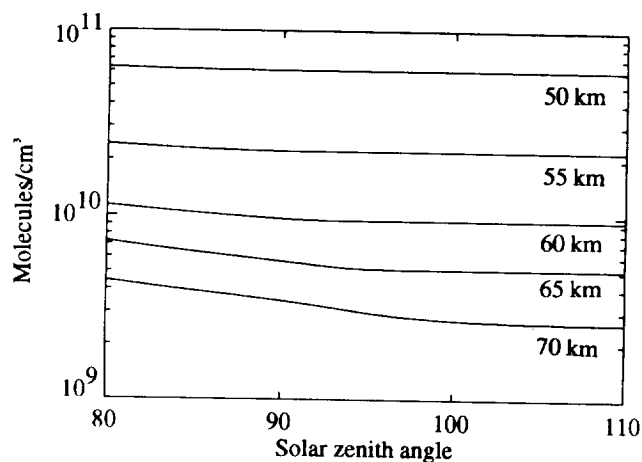


Fig. 2 The calculated variation of odd oxygen of $\text{HO}_x\text{-O}_x$ chemistry at sunset between 80° and 110° solar zenith angle from 50 to 70 km altitude.

Table 2 Selected days of SAGE II ozone observations

	sunrise	sunset
Nov 6	21.3° N	21.3° N
Jan 16 & 17	17.5° N	17.1° N
May 6 & 7	20.7° S	21.5° S
July 18	17.0° S	17.8° S

Figures 3(a) and 3(b) show the variation of ozone between 80° and 110° solar zenith angles during sunset and sunrise, respectively. The modeled ozone variations for both sunset and sunrise show good agreement with Allen et al (1984).

OH oscillates up and down within the two-hour period around sunset at 70 km. Figure 4 illustrates the OH variations with solar zenith angle. The variations of HO_2 (not shown) are photochemically coupled with OH. The variations of OH are less important during the period before sunrise (not shown) than in the period after sunset not only because OH concentrations are approximately an order magnitude smaller but also because the abundances of atomic oxygen are small. Therefore the destruction of O_x due to HO_x is not effective just before sunrise, and only the conversion of ozone to atomic oxygen needs to be considered in this period.

The photodissociation of water vapor is not included in the model because (1) the photodissociation of H_2O is quite small at twilight in the mesosphere and (2) there is no direct impact on O_3 due to H_2O . In addition, SAGE II does not measure H_2O above the stratosphere. Furthermore, we would like to keep the photochemical reaction set as simple as possible in order to better understand the photochemistry in the mesosphere. The results indicates that at 70 km a 5% OH change will induce a 1% change in O_3 . The one hour average of $J_{\text{H}_2\text{O}}$ before sunset contributes approximately 5% increase in OH. Therefore 1% ozone change is expected. But this can be neglected compared to SAGE II measurement uncertainty.

The comparisons of model results and SAGE II ozone measurements

Because of seasonal and latitudinal variations in the ozone diurnal changes, the selection of SAGE II measurements used in the comparison becomes significant. In one year of SAGE II data, only five days (four days in tropical region and one at mid-latitude) have been found where sunrise and sunset events are within one degree of latitude difference in a 24 hour period. Table 2 exhibits selected profiles when the average zonal mean

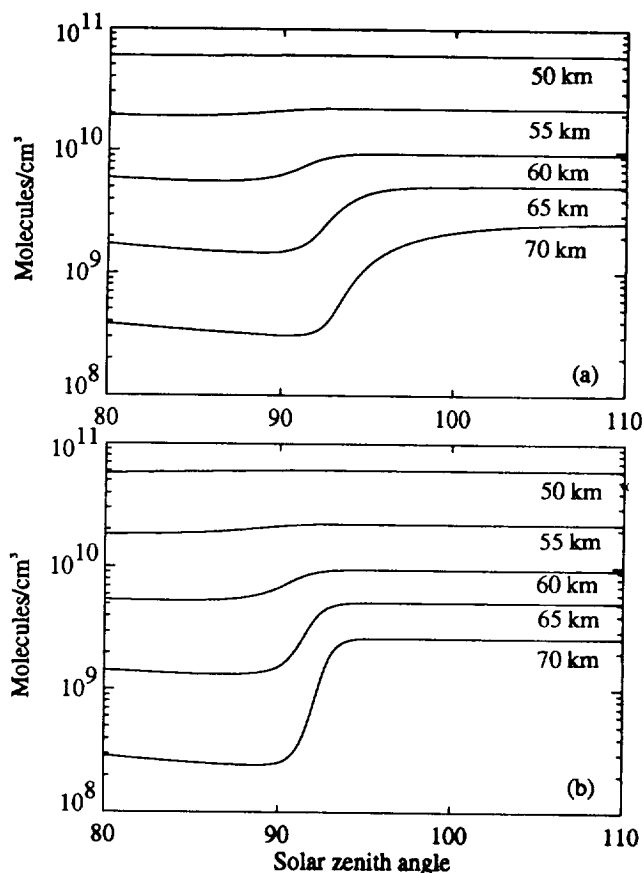


Fig. 3 (a) The calculated variation of ozone of $\text{HO}_x\text{-O}_x$ chemistry at sunset between 80° and 110° solar zenith angle from 50 to 70 km altitude. (b) same as (a) except at sunrise.

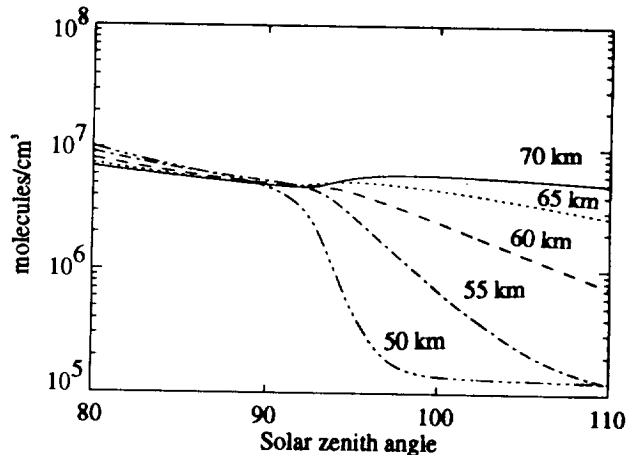


Fig. 4 The calculated variation of OH of $\text{HO}_x\text{-O}_x$ chemistry at sunset between 80° and 110° solar zenith angle from 50 to 70 km altitude.

latitudes of sunrise and sunset events are within 1 degree of each other. In this comparison, only SAGE II zonal mean values are used. The longitudinal variation of the ozone measurements is affected by random noise (Cunnold et al, 1984 and 1989) particularly in the tropical region - where most of the sunrise and sunset coincidences occur.

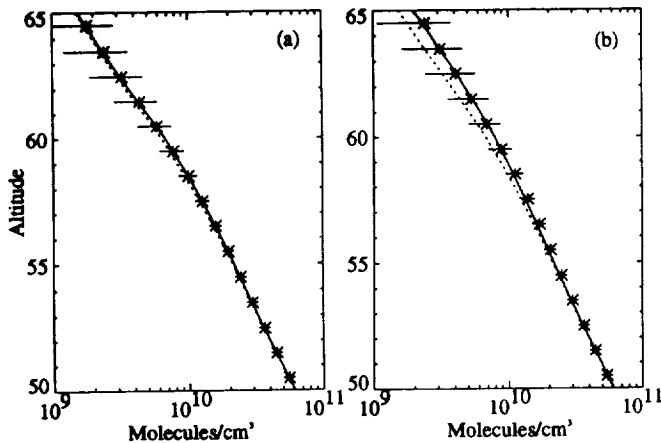


Fig. 5 (a) The comparisons of ozone profiles on the selected days between 50 and 65 km at sunset; star with error bar : SAGE II ozone profile; solid line : retrieved ozone profile of model results; dotted line : ozone profile at 90° solar zenith angle of model results. (b) same as (a) except at sunrise.

Within the four tropical zonal means, it is found that the model results display nearly identical ozone variations both at sunrise and sunset. Therefore the ensemble mean of the zonal average of the four coincident events (per year) can be used to compare with the model predictions. Figures 5(a) and 5(b) shows the means (star) and standard deviations (shown as error bars) of the twenty events at both sunrise and sunset of the selected days over the five-year SAGE II data set. In the calculations reported here SAGE II sunset profiles have been used as a constraint on the ozone near 90° solar zenith angle.

An onion-peeling algorithm applied to slant column inferred from the model results begins at 78 km (ozone at 78 km is guessed initially). The ozone concentration is estimated by subtracting the sum of the ozone concentrations weighted by the path length in all higher altitude layers from the slant column content. In the onion peeling inversion, homogeneous spherical shells with constant ozone concentrations are assumed. This procedure produces a hypothetical ozone profile inferred from the model calculations which may be directly compared against retrieved SAGE II ozone profiles.

For pure oxygen chemistry the modeled and observed sunrise/sunset ratio agrees well only at the altitudes between 50 and 60 km. Overestimates of the ratio are found above 60 km with a maximum of 30% at 63 km. The overestimation is totally attributable to the excess of oxygen atoms above 60 km in the model at sunset, which then produce excessive nighttime ozone concentration. Consequently an excessively large and asymmetric ozone variation is produced at sunrise. Because the asymmetry will propagate downward via the onion peel procedure, the more asymmetric the variation about 90° the deeper the effect will penetrate.

When the chemistry of odd oxygen and odd hydrogen is included, fewer oxygen atoms are available to be converted into ozone and therefore there is a tendency for an increase in the ozone photodissociation rate. At 70 km, the transition from O to O₃ is thus deferred at sunset, and an earlier transition occurs oppositely at sunrise. The time difference corresponds to approximately one degree solar zenith angle. At lower altitudes because of the smaller ozone diurnal variation the effect is less pronounced.

Figures 5(a) and 5(b) have also displayed the simulated ozone (i.e. the solid lines) after the onion-peeling retrieval method has been applied. The agreement between SAGE II

Table 3 Correction factors of SAGE II ozone profiles at sunrise and sunset in the tropics

km	65	64	63	62	61	60	59	58	57	56	55
sr	1.29	1.30	1.29	1.26	1.21	1.16	1.12	1.09	1.06	1.03	1.03
ss	1.03	1.04	1.05	1.06	1.07	1.07	1.07	1.06	1.06	1.04	1.03

sr : sunrise; ss : sunset

ozone means and modeled ozone is within 1% at sunset and better than 5% at sunrise. We consider these difference to be small compared to the measurement uncertainties of SAGE II. Furthermore, the photochemical reactions used in the model, disregarding the photodissociation of water vapor, are sufficient to describe sunset and sunrise ozone variations in the altitudes from 50 to 65 km.

Also, in Figures 5(a) and 5(b) the ozone values at 90° solar zenith angle are shown as dotted line. According to the ozone profiles at 90° solar zenith angle and the simulated ozone profile (at which the onion-peeling method has been applied), we can infer the correction factors for the SAGE II ozone measurements. Table 3 shows the correction factors between 55 and 65 km. Below 55 km only 1% corrections are needed.

Acknowledgements

Thanks to W. P. Chu at NASA Langley Research Center for his informative suggestions. This work is under NASA contract NAS1-18487.

References

- Allen, M., J. I. Lunine and Y. L. Yung, The vertical distribution of ozone in the mesosphere and lower atmosphere, *J. Geophys. Res.*, 89, 4841-4872, 1984.
- Anderson, D. E., The troposphere-stratosphere radiation field at twilight : A spherical model, *Planet. Space Sci.*, 31, 1517-1523, 1983.
- Atmospheric Ozone, 1985
- Chu, D. A., The interpretation of SAGE II ozone measurements in the lower mesosphere, Ph.D. thesis, 110pp, Georgia Institute of Technology, Atlanta, Georgia, June 1989.
- Chu, W. P., M. P. McCormick, J. Lenoble, C. Brogniez and P. Pruvost, SAGE II inversion algorithm, *J. Geophys. Res.*, 94, 8339-8351, 1989.
- Cunnold, D. M., W. P. Chu, R. A. Barnes, M. P. McCormick, R. E. Veiga, Validation of SAGE II ozone measurements, *J. Geophys. Res.*, 94, 8447-8460, 1989.
- Frederick and Hudson, 1980, Dissociation of molecular oxygen in Schuman-Runge bands, *J. Atmos. Sci.*, 37, 1099-1106.
- Noxon, J. F., E. C. Whipple, Jr., and R. S. Hyde, Stratospheric NO₂, 1, Observational method and behavior at mid-latitude, *J. Geophys. Res.*, 84, 5047-5063, 1979.
- Prather, M. J., Ozone in the upper stratosphere and mesosphere, *J. Geophys. Res.*, 86, 5325-5338, 1981.
- Rusch, D. W. and S. C. Liu, The effects of recent solar flares measurements and water vapor dissociation calculations on mesospheric chemistry, in Proceeding Quadrennial International Ozone Symposium, edited by J. London, pp. 869-875, International Ozone Commission, Boulder, Col., 1981.
- Smith, F. L. III and C. Smith, Numerical evaluation of Chapman's grazing incidence integral ch(X,c), *J. Geophys. Res.*, 77, 3592-3597, 1972.
- Solomon, S. A. L. Schmeltekopf, R. W. A. Sanders, On the interpretation of zenith sky absorption measurements, *J. Geophys. Res.*, 92, 8311-8319, 1987.
- U. S. Standard Atmosphere, Washington DC, October 1976.